Proceedings of the 2025 Design of Medical Devices Conference
DMD2025
April 28-30, 2025, Minneapolis, MN, USA

DMD2025-1096

GaitWay: Development and Testing of a Novel Ambulation Device for Gait Rehabilitation

Leah Thomas, B.S.*
Virginia Tech
Roanoke, VA

Andrew Schroeder, M.D*
Carilion Clinic &
Virginia Tech
Roanoke, VA

Jenna Altaii, B.S.*
Virginia Tech
Roanoke, VA

Dr. Robert Stone, Ph.D.
Virginia Tech
Blacksburg, VA

Dr. Arnold D. Salzberg, M.D.
Carilion Clinic
Roanoke, VA

Dr. Christopher B. Arena, Ph.D.
Virginia Tech
Blacksburg, VA

**Authors contributed equally to this work.*

Abstract

Approximately 7–12% of the U.S. population experiences significant ambulation limitations, yet rural areas face a 50% shortage of physical therapists per capita. This disparity, combined with the risks and challenges associated with prolonged immobility, underscores the need for innovative solutions to simulate the benefits of walking without the risks of standing. While existing therapies like early mobilization and passive exercises improve outcomes, they often rely on extensive personnel support, limiting accessibility in resource-constrained settings. The proposed device provides bedridden patients simulated walking mechanics and neuromuscular pathway training to address the challenges they face. This study focuses on bench validating the performance of the motor used to power the device. Controlled tests assessed the performance under torque control and resulted in a function that determines output force based on input load weights and motor control values. These results validate the chosen electrical and mechanical components for the system's further development.

Keywords: ambulation, gait training, biomechanics, physical therapy, rehabilitation device

1. INTRODUCTION

7-12% of the U.S. population experiences significant ambulation limitations [1,2]. The healthcare sector employs over 500,000 physical therapists who deliver approximately 300 million therapy sessions annually [3]. Despite this national workforce, rural areas experience a significant gap, with 50% fewer therapists per capita compared to urban centers [4]. Through the process of clinical immersion and needs assessment, we determined an unmet need for a way to simulate the benefits of walking without the risks of standing.

Immobility contributes to poor patient outcomes. Daily bed rest can cause a 1.3–3% decline in muscle strength in healthy individuals [5]. Across multiple patient populations, early ambulation has been shown to decrease length of hospital stays and post-operative risks [6,7,8,9]. Despite these benefits, safety concerns performing ambulation training with ventilated patients can lead to neglect and increased risk of complications [10,11]. Ambulation training also requires significant resources and qualified staff, which are often limited. Therefore, innovative solutions are needed to reduce time to independent walking, dependence on personnel, and risks associated with standing.

Several devices offer ambulation training but have notable limitations. The PhysioGait helps patients maintain posture and reduces load but requires assistance during use. The HealthStep Recumbent Stepper can be used in bed but must be used sitting upright. LegXercise improves mobility but only provides passive exercise. Other upcoming solutions cannot be used supine, do not provide biofeedback, or do not offer an incremental range of assistance from passive to fully active exercise [12]. Our device, the GaitWay, targets patients with limited mobility to provide a range of exercise, providing biofeedback and training gait while supine.

2. MATERIALS AND METHODS

2.1 User Needs and Design Input

Subject Matter Expert (SME) interviews helped the team determine a series of user needs and design inputs (Table 1).

TABLE 1: User Needs and Design Inputs

User Needs	Design Inputs	Source
Device promotes activation of muscle groups in the same pattern as walking	The device shall facilitate the activation of key lower-limb muscle groups in a pattern that replicates the typical activation sequence measured by EMG during normal gait cycles	SME Interview
Device improves muscle strength	Device shall increase lower-limb muscle strength (measured as peak torque in quadriceps and hamstrings) by at least the expected strength increase to ambulate from standard PT	SME Interview
Device includes features that focus on cardio	Device shall elevate and sustain user's heart rate to at least 50-85% of age-predicted max heart rate for a min of 10 minutes per session	[13]
Device includes method for collecting objective quantitative data of patient progress	Sensor data will be collected for 30 mins of treatment and compared to proper gait cycle to calculate "deviation score"	SME Interview
Device provides range from fully passive to fully active	Device may be operated with an adjustable assistive force proportional to the force exerted by patients	SME Interview

2.2 Device Design

The GaitWay is designed to be positioned at the foot of a bed, perpendicular to the bedframe, enabling bedbound patients to use it while supine. It features a plate that directly attaches to each foot allowing full range of motion throughout the gait cycle (purple arrows in Fig. 2). The footplate will be on a rail mechanism approximately 1.3 m in length to match the average stride length [14]. A separate larger plate behind the footplate will provide a simulated ground reaction force (green arrows in Fig. 1 and 2).

FIGURE 1: SCHEMATIC OF PATIENT USING DEVICE

The device simulates real-life stepping mechanics by providing dynamic force adjustments throughout the walking cycle, engaging coordinated muscle activity, and retraining neuromuscular pathways. The duration and level of exercise can be adjusted to accommodate the user's current mobility status. This device is designed to replicate the forces experienced during independent walking while also providing an adjustable assistive force for patients who require additional support. Its customizable therapeutic range ensures accessibility for patients of all abilities, making the therapy versatile and inclusive. Using the system has the potential to reduce the time to independent ambulation and the risk of permanent disability. Future work will determine device dimensions and other motion limits.

The GaitWay must achieve two goals: to counteract the weight of the leg due to gravity, which would be negligible when walking upright, and to provide an assistive force proportional to the force exerted by patients who do not have the strength to operate the device unassisted. Fig. 3 describes the system architecture for guiding the device response. The known weight of the leg (W_l) and force sensor data from the user's foot (F_a, F_h, F_d, F_p) are used to estimate the user's exerted force on the device (F_u). A normalized table of expected forces to position (E_e), based on the user's height and weight, is used to compare the expected force for a specific position to the user's position and force data (E_u). An assistive multiplier A is calculated as a value proportional to (E_e / E_u), which calculates the final force the motor applies on the user's foot. In our simplified system focusing only on forces along the axis of gravity, these forces can be represented as a single equation:

$$F_f = W_l + A(W_l - F_h) \quad (1)$$

where F_f is the force acting on the user's foot, W_l is the weight of the user's leg, F_h is the force read at the user's heel (a measure of the user's effort to lift their leg upwards), and A is the assistance multiplier. The assistive force represented by A in Eq. (1) plays a pivotal role in dynamically enhancing the user's effort during the gait cycle. This force multiplier amplifies the force exerted by the user ($W_l - F_h$), effectively lowering the physical demand required to lift the leg and complete a step. The assistive force bridges the gap between the user's voluntary effort and the biomechanical load necessary for gait, ensuring engagement even with insufficient user muscular output. The value of A can be manually adjusted based on clinical judgment or automatically modulated by the system in response to real-time user performance by intermittently assessing the ability of a user to progress through a gait cycle and increasing A. Conversely, clinical judgment or the system can progressively decrease A to progress the user's strength training. To prevent excessive force, A would be capped at physiologic walking forces. To test the selection of our prototype's mechanical and electrical components, we focused on a single vertical axis of movement as a simplified representation of our system.

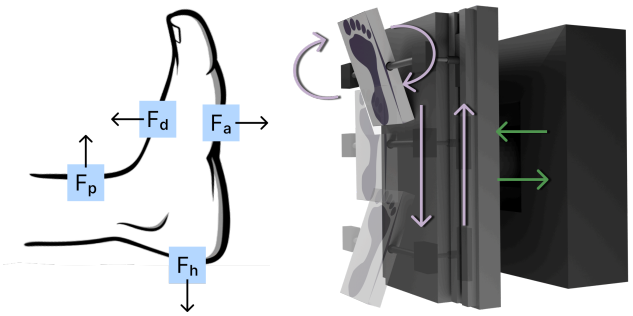

FIGURE 2: FORCE SENSOR PLACEMENT AND PROPOSED DEVICE MODEL
Foot force sensors: Fh (heel), Fa (anterior ankle) Fp (plantar), Fd (dorsal).

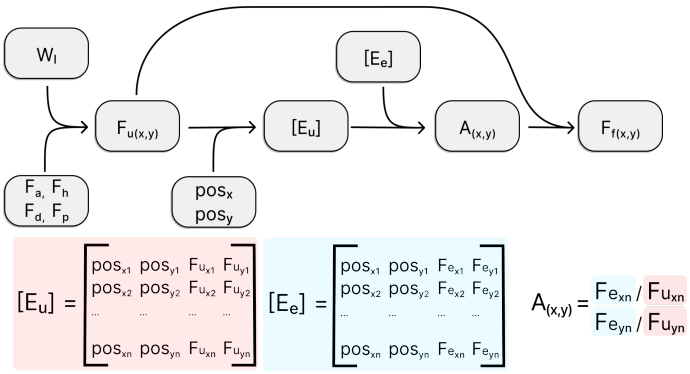

FIGURE 3: GAITWAY SYSTEM ARCHITECTURE

2.3 Device Components

The electronic components of the device prototype consist of a microcontroller (ESP32-DEVKITM-1, Espressif Systems), a brushless DC motor (BLDC)(QBL5704-116-04-042, Trinamic), a breakout board (TMC4671+TMC6100 BOB, Analog Devices), and an AC/DC converter (AMES200-36SNZ-Q, Aimtec) (Fig. 4).

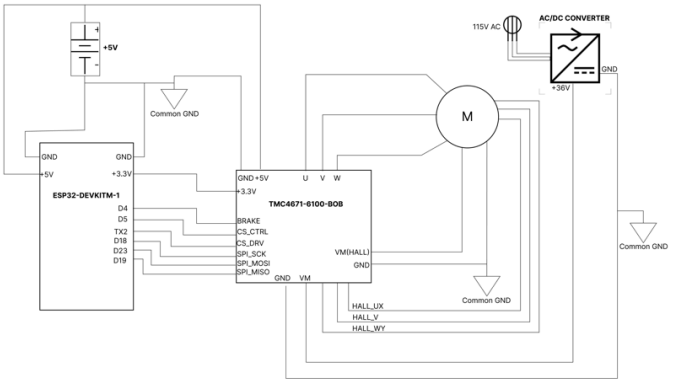

FIGURE 4: CIRCUIT DIAGRAM

The mechanical components consist of a v-slot linear rail (20x20mm), 6mm and 8mm bore pulleys, a 5M GT2 Timing Belt, and a 20mm V Gantry Plate creating a platform to hold weights for testing.

2.4 Motor Current Draw Testing Methods

A series of controlled tests were conducted to characterize the BLDC motor's output and operational capabilities under torque control mode, evaluate its performance, and validate the chosen components' suitability for the device.

Electrical current was measured on the DC supply line (V_{in}) feeding the motor controller. An AC/DC current clamp (CC-65, Hantek) was used to record the input current at a sampling rate of 100Hz on an oscilloscope. The supply voltage was measured at 36V. Digital motor control values (DMCV) of T = 2000 and T = 4000 were tested in three trials each. These values were chosen as the minimum input value to the motor controller to lift the weights at a reasonable acceleration. To facilitate comparison, a common time vector was created for each condition ranging from t=0 to t=T_{avg} (the mean trial duration). The three current datasets per DMCV were smoothed using a moving average filter in MATLAB, spline-interpolated onto the common time vector, and then averaged pointwise to yield a representative *I(t)* profile. Instantaneous electrical input power (P_{in}) was calculated by multiplying the averaged current profiles by the supply voltage. The total electrical energy consumption of the system (E_{in}) was computed using numerical trapezoidal integration of P_{in} over the trial duration. Using the data from Section 2.5, average acceleration values for each trial were multiplied by the common time vector to create an approximate velocity profile. The force of the load moving up the rail was calculated assuming negligible friction and multiplied by the velocity profile to compute the mechanical power of the system (P_{out}). Finally, the mechanical energy output (E_{out}) was obtained by integrating P_{out} over the time interval.

2.5 Motor Torque Testing Methods

The prototype device was vertically secured for stability during testing. A BLDC motor drove a belt system to lift a plate with incremental weights, tracked using a measurement scale aligned with the belt's path (Fig. 5). High-speed video captured positional and temporal data for precise frame-by-frame analysis. Weights on the plate varied and displacement over time was recorded. A second-order polynomial regression of the displacement-time curve yielded an $R^2 > 0.999$, confirming uniform acceleration driven by motor torque. Acceleration was computed using kinematic equations and validated via the second derivative of the polynomial. Force was calculated using acceleration and mass, assuming idealized conditions without accounting for losses like friction or belt elasticity (Eq. (2)).

$$F_f = m(g+2h/t^2) \quad (2)$$

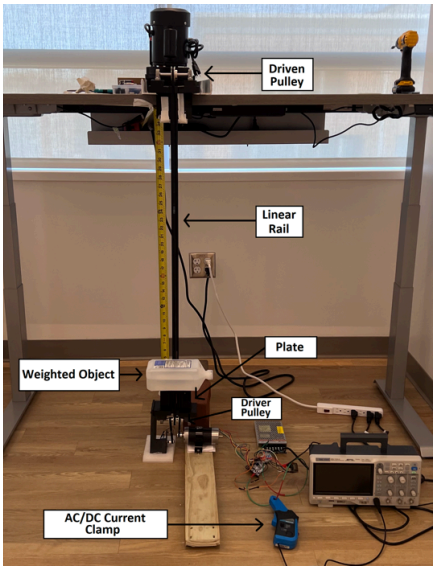

FIGURE 5: EXPERIMENT TEST SETUP

3. RESULTS AND DISCUSSION

3.1 Motor Current Draw Analysis

The DMCVs were tested to investigate their effects on the system's current draw, power consumption, electrical energy, and mechanical output when lifting a 1 lb mass to a height of 0.77 m on a linear rail. As demonstrated in Fig. 6, under the T=4000 condition, current spikes reached a peak of 1.54 A, whereas T=2000 had lower current peaks (0.76 A) but a significantly longer duration, approximately double that of T=4000. Consequently, the average current for T=4000 (0.50 A) exceeds T=2000 (0.30 A), even though the total operation time was shorter for T=4000.

In both conditions, the observed negative current spikes before the peak are likely caused by back-electromotive force (back-EMF) generated during rapid transitions. Back-EMF occurs when the voltage induced in the motor windings opposes the externally applied voltage that drives the motor [15]. In torque control mode, the motor driver actively adjusts the current to maintain the target torque, making the system highly responsive to load changes. During the rapid acceleration of the load moving up the rail, back-EMF can momentarily exceed the supply voltage, causing brief current reversals as energy flows back into the system. These spikes are an expected artifact of the interaction between the motor's back-EMF and the TMC4671+TMC6100 motor driver's current adjustments inherent in torque control mode [15]. MOSFET switching refers to the rapid turning on and off of metal-oxide-semiconductor field-effect transistors (MOSFETs) to regulate power delivery to the motor, influencing efficiency, heat dissipation, and electromagnetic interference. Future trials will include optimizing parameters in the motor driver, such as adjusting the break-before-make (BBM) timing logic to prevent shoot-through, fine-tuning the gate drive strength to control MOSFET switching speed, and adding additional bulk capacitance if needed [14].

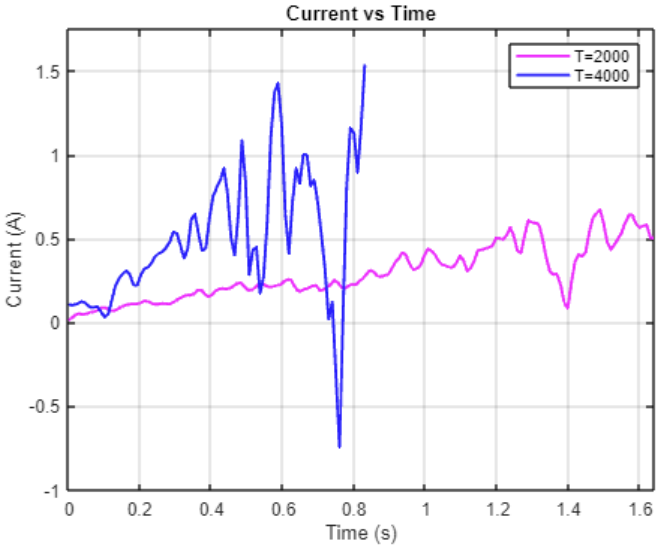

FIGURE 6: CURRENT VS. TIME DATA

Bar charts of maximum instantaneous power and average power (see Fig. 7) indicate that T=4000 nearly doubles the peak power draw (55.44 W vs. 27.28 W) and exceeds the average power (18.02 W vs. 10.75 W) relative to T=2000. Despite its higher instantaneous power usage, T=4000 completes the lift in less time and subsequently draws less total electrical energy (14.84 J) than T=2000 (17.92 J). The longer current duration under T=2000 accounts for higher total energy use despite lower instantaneous power. These results indicate that applying a higher DMCV shortens the lift duration sufficiently to reduce the overall energy intake at the DC supply side. The QBL5704 motor datasheet confirms that the measured results lie within the motor's capabilities but in a lower-torque regime [16]. The measured peak power (up to ~55 W) is well below the motor's maximum theoretical capability (peak current of 20.5 A * 36 V input voltage = 738 W) suggesting that future tests can explore higher DMCVs to improve energy efficiency further [17].

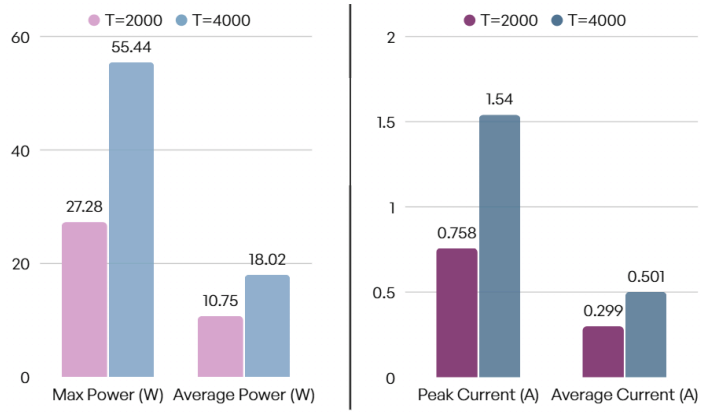

FIGURE 7: MAX POWER, AVERAGE POWER, PEAK CURRENT, AND AVERAGE CURRENT VALUES

Electrical energy input and mechanical energy output are compared in Fig 8. With T=2000, the system outputs 3.78J mechanically while consuming 17.92 J electrically (~21% efficiency). Under T=4000, the mechanical output increases slightly to 4.31 J but requires only 14.84 J of electrical energy (~29% efficiency). Therefore, T=4000 not only uses less total electrical energy but also converts a larger fraction of it into useful work. These results suggest that T=4000 operates in a more optimal torque-speed range, closer to the motor's rated performance, however, future trials should aim to optimize parameters to reach a higher efficiency of at least 75%.

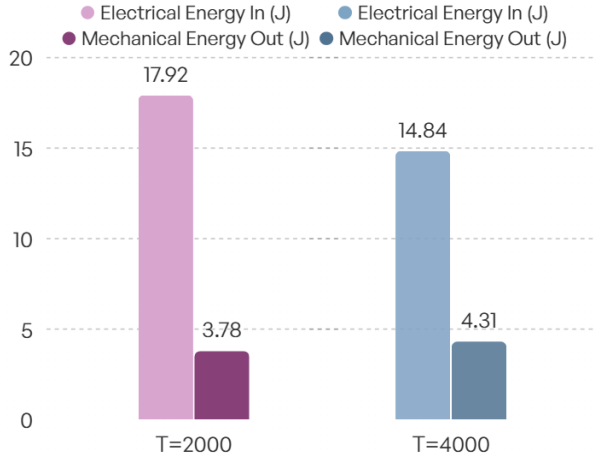

FIGURE 8: CALCULATED ELECTRICAL ENERGY AND MECHANICAL ENERGY CONSUMPTION

In summary, T=4000 shows higher instantaneous current and power but achieves lower total energy consumption and higher mechanical efficiency than T=2000. Although larger current spikes require adequate thermal management, the overall energy usage is lower and more efficient. These findings highlight a trade-off between peak current handling and overall efficiency, demonstrating that higher DMCVs can raise the peak power/current but shorten the overall lift duration, improving total efficiency and reducing total energy drawn.

Future testing will include evaluating higher DMCV to assess the motor characteristics under higher torque and current conditions. Additionally, trials with heavier weights will determine the motor's operational limits, while implementing a larger gear ratio will enable higher torque output for larger loads. A torque sensor on the output shaft will assess the system's mechanical energy and efficiency measurements. These tests will aid in creating an optimization algorithm for BLDC input parameters, which will maximize system efficiency based on the weight of the patient's leg.

3.2 Motor Torque Analysis

The motor torque testing successfully characterized the relationship between the DMCV and the force exerted on the footplate across varying load conditions. As expected, heavier loads on the system resulted in lower acceleration magnitude and higher force magnitude. T=4000 resulted in greater acceleration and force values compared to T=2000, which is consistent with the results reported in Table 2 summarizing the relationship between DMCV, load weight, average acceleration, and force.

TABLE 2: Forces of Various Loads and DMCVs

DMCV	Weight (lb)	Avg Acceleration (m/s^2)	Force (N)
2000	1	0.574902267	4.710508589
	2	0.243986386	9.120815585
	3	0.06948831	13.34921256
4000	1	2.283251971	5.485402348
	2	1.764560201	10.50025582
	3	0.491993629	14.01870568

Using data from systematically increasing load weight and recording displacement and motor input, a mathematical function (see Fig. 9) was developed to map the load weight and DMCV to the force generated at the footplate, achieving a high correlation (R^2 value >0.99). This function enables precise adjustment of motor output. This precision is key for having the motor respond to the patient's effort, ensuring appropriate counteraction of gravity and assistive force delivery throughout the gait cycle.

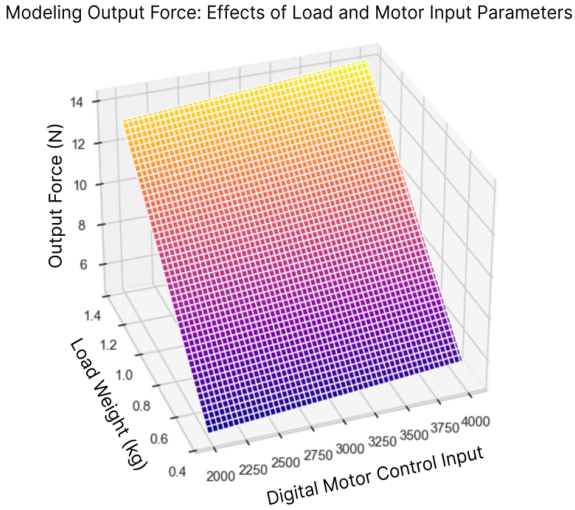

FIGURE 9: MAPPING OF WEIGHT AND DMCV TO FORCE

Future tests will evaluate higher DMCV values, gather precise position data, test larger weights, and verify results with torque sensors and tension gauges. These results will help build a mathematical model that maps the relationship between digital input, load weight, and resulting force on the linear rail system. This model will be crucial for developing the GaitWay's control architecture. By characterizing how digital input correlates with physical output, the system can dynamically adjust to patient-specific requirements, simulating real-time gait patterns across a spectrum of mobility levels. This function aids in determining the optimal input parameters for the device to

apply an assistive force accurately. This transforms the GaitWay from a passive rehabilitation device to an adaptive responsive system capable of supporting a wide spectrum of patients, from those requiring minimal passive movement to those progressing towards independent ambulation.

3.3 Limitations

Several assumptions and factors during testing may have influenced the results. First, the belt tension may have varied between trials due to prior testing or displacement caused by the plate's impact with the top of the linear rail. Additionally, the calculations assumed a frictionless, drag-free system, whereas friction was present at multiple points such as the motor and pulley system. Finally, only the start/end position and flight time were recorded for each trial. Inaccurate time synchronization between current and velocity measurements may have affected mechanical energy calculation accuracy.

4. CONCLUSION

The results of the controlled bench testing validate the motor's performance under torque control. Higher DMCVs lead to improved efficiency, increased instantaneous power and current, and decreased total energy consumption. The developed function accurately maps digital input and load weight to force output, allowing control of the assistive force delivery. Future work will include incorporating a higher gear ratio to accommodate heavier weight, developing a high-fidelity prototype for human-subject testing, and creating a predictive mathematical model to optimize the performance of the system and calculate the assistive force needed by each patient. By integrating a proportional assistance mechanism, the final device will personalize therapy, accelerate functional recovery, and reduce reliance on continuous therapist intervention. Validation will start with healthy subjects testing. We will then conduct a pilot study on bed-bound patients to evaluate clinical efficacy. The goal of the final device is to simulate walking with high enough fidelity that patients can progress in their ability to walk faster, validated by the time taken to independent ambulation.

ACKNOWLEDGEMENTS

Thanks to Dr. Sara Arena and Dr. Robin Queen for their guidance and the Physical Therapy teams at Carilion Clinic and Warm Hearth for facilitating clinical immersion.

REFERENCES

[1] A. Geiger, "8 facts about Americans with disabilities," Pew Research Center, Apr. 14, 2024. [Online]. Available: https://www.pewresearch.org/short-reads/2023/07/24/8-facts-about-americans-with-disabilities/
[2] "Disability impacts all of us Infographic | CDC," Centers for Disease Control and Prevention, May 15, 2023. https://www.cdc.gov/ncbddd/disabilityandhealth/infographic-disability-impacts-all.html
[3] S. Zauderer, "59 Physical Therapy Statistics, Facts & Demographics," Jul.23,2023. https://www.crossrivertherapy.com/research/physical-therapy-statistics
[4] NCHWA, "Distribution of U.S. health care providers residing in rural and urban areas." [Online]. Available: https://www.ruralhealthinfo.org/assets/1275-5131/rural-urban-workforce-distribution-nchwa-2014.pdf
[5] R. Topp, et al., "The effect of bed rest and potential of prehabilitation on patients in the intensive care unit," AACN Clinical Issues, vol. 13, no. 2, pp. 263–276, May 2002, doi: 10.1097/00044067-200205000-00011.
[6] O. Adogwa et al., "Early ambulation decreases length of hospital stay, perioperative complications and improves functional outcomes in elderly patients undergoing surgery for correction of adult degenerative scoliosis," Spine, vol. 42, no. 18, pp. 1420–1425, Apr. 2017, doi: 10.1097/brs.0000000000002189.
[7] L. M. Fleming *et al.*, "Early ambulation among hospitalized heart failure patients is associated with reduced length of stay and 30-Day readmissions," *Circulation Heart Failure*, vol. 11, no. 4, Apr. 2018, doi: 10.1161/circheartfailure.117.004634.
[8] L. B. Oldmeadow et al., "NO REST FOR THE WOUNDED: EARLY AMBULATION AFTER HIP SURGERY ACCELERATES RECOVERY," *ANZ Journal of Surgery*, vol. 76, no. 7, pp. 607–611, Jun. 2006, doi: 10.1111/j.1445-2197.2006.03786.x.
[9] P. Talec, et al, "Early ambulation and prevention of post-operative thrombo-embolic risk," *Journal of Visceral Surgery*, vol. 153, no. 6, pp. S11–S14, Oct. 2016, doi: 10.1016/j.jviscsurg.2016.09.002.
[10] W. D. Schweickert et al., "Early physical and occupational therapy in mechanically ventilated, critically ill patients: a randomized controlled trial," Lancet, vol. 373, no. 9678, pp. 1874–1882, May 2009, doi: 10.1016/s0140-6736(09)60658-9.
[11] "The role of polyneuropathy in motor convalescence after prolonged mechanical ventilation," PubMed, Oct. 18, 1995. https://pubmed.ncbi.nlm.nih.gov/7563512/
[12] F. M. Lim *et al.*, "Supine GAIT Training Device for stroke Rehabilitation – Design of a compliant ankle orthosis," Springer International Publishing Switzerland, 2014. doi: 10.1007/978-3-319-02913-9_130.
[13] "Exercise intensity: How to measure it," *Mayo Clinic*. https://www.mayoclinic.org/healthy-lifestyle/fitness/in-depth/exercise-intensity/art-20046887
[14] A. Peruzzi, et al, "Estimation of stride length in level walking using an inertial measurement unit attached to the foot: A validation of the zero velocity assumption during stance," Journal of Biomechanics, vol. 44, no. 10, pp. 1991–1994, May 2011, doi: 10.1016/j.jbiomech.2011.04.035.
[15] S. Keeping, "Controlling sensorless BLDC motors via back EMF," DigiKey, Jun. 19, 2013. https://www.digikey.com/en/articles/controlling-sensorless-bldc-motors-via-back-emf
[16] Trinamic, "TMC4671+TMC6100 BOB Description." TMC4671+TMC6100 BOB datasheet, Jan. 2020.
[17] Trinamic, "QMot QBL5704 family." QBL5704 manual, Aug. 2020.